ORIGINAL PAPER

Exploring the binding pocket for pyridopyrimidine ligands at the CCK1 receptor by molecular docking

**Amel Toumi-Maouche · Boubekeur Maouche ·
Safia Taïri-Kellou · Salima El-Aoufi ·
Mercedes Martín-Martínez · Rosario González-Muñiz ·
Daniel Fourmy · Bernard Maigret**

Abstract Pyridopyrimidine-based analogues are among the most highly potent and selective antagonists of cholecystokinin receptor subtype-1 (CCK1R) described to date. To better understand the structural and chemical features responsible for the recognition mechanism, and to explore the binding pocket of these compounds, we performed automated molecular docking using GOLD2.2 software on some derivatives with structural diversity, and propose a putative binding conformation for each compound. The docking protocol was guided by the key role of the Asn333 residue, as revealed by site directed mutagenesis studies. The results suggest two putative binding modes located in the same pocket. Both are characterized by interaction with the main residues revealed by experiment, Asn333 and Arg336, and differ in the spatial position of the *Boc*-Trp moiety of these compounds. Hydrophobic contacts with residues Thr117, Phe107, Ile352 and Ile329 are also in agreement with experimental data. Despite the poor correlation obtained between the estimated binding energies and the experimental activity, the proposed models allow us to suggest a plausible explanation of the observed binding data in accordance with chemical characteristics of the compounds, and also to explain the observed diastereoselectivity of this family of antagonists towards CCK1R. The most reasonable selected binding conformations could be the starting point for future studies.

Keywords Cholecystokinin · CCK receptor antagonists · Docking · Molecular modeling

A. Toumi-Maouche (✉) · B. Maouche · S. Taïri-Kellou ·
S. El-Aoufi
Laboratoire de Physico-Chimie Théorique et Chimie Informatique,
Faculté de CHIMIE,
USTHB B.P. 32, El Alia, Alger, Algeria
e-mail: ameltoumi_usthb@yahoo.fr

M. Martín-Martínez · R. González-Muñiz
Instituto de Química Médica (CSIC),
Juan de la Cierva 3,
28006 Madrid, Spain

D. Fourmy
Equipe de Biologie et Pathologie Digestive, INSERM U531,
Institut Louis Bugnard, CHU Rangueil,
Bâtiment L3,
31403 Toulouse cedex 4, France

B. Maigret
Laboratoire Lorrain de Recherche en Informatique et ses Applications,
LORIA-615, Rue du Jardin Botanique,
54600 Villers Les-Nancy, France

Introduction

Understanding the interactions between ligands and their target receptor is an essential step in any pharmaceutical or chemical research program. Although clearly helpful in the development of new therapeutic molecules, this area represents a great challenge in the drug design field. Experimental techniques such as fluorescence spectroscopy, photoaffinity labelling, nuclear magnetic resonance, x-ray or site directed mutagenesis, are used to provide information about the environment of a ligand within the binding site, as well as in the analysis of conformational changes in the target receptor and motion that occurs upon activation [1–5]. However, these methods are often difficult, or even impossible, due to the limited availability of protein targets, especially in the G-protein coupled receptor (GPCR) field. Computer-aided simulation of protein–ligand interactions using molecular modeling tools can often be of great help in guiding and interpreting experiments, and is helpful in providing atomic details that are inaccessible using other

experimental techniques [6]. Therefore, the combination of molecular modeling and experimental analysis can provide much detailed information speeding the drug discovery process, and has become essential in any de novo design process. Generally, in computer-aided drug design, two principal approaches are used: ligand-based drug design [7] and structure-based drug design [8, 9].

In this context, we were interested in the application of a structure-based strategy to explore the molecular recognition mechanism between a series of pyridopyrimidine derivatives and the binding site of a transmembrane GPCR—subtype-1 of the cholecystokinin receptor (CCK1R) [10–12]. Previous studies have shown the high binding affinity and potent antagonist activity of these compounds towards rat CCK1R [13–16]. CCK1R is one of two receptors mediating the physiological action of cholecystokinin (CCK) [10–12], an important endogenous neuropeptide hormone well known to be involved in many biological actions, such as regulation of pancreatic enzyme secretions, gallbladder contraction, colonic motility and satiety control [17, 18]. CCK1Rs are localized mainly in the gastrointestinal tract, where they are involved in diverse digestive processes [10–12].The therapeutic potential of CCK1R antagonists in treating CCK-related disorders has stimulated extensive research into small non-peptide ligands, and different strategies have been used for the discovery of several classes of compounds with high structural diversity [19, 20]. The pyridopyrimidine-based lead IQM—95,333 (2a) is one of the most selective CCK1R antagonists described to date, both in vitro and in vivo [21]. It was obtained by replacement of the key Met[31]–Asp[32] fragment of the endogenous ligand CCK-4 (Trp[30]-Met[31]-Asp[32]-Phe[33]-NH$_2$), by a 5-amino-1,3-dioxoperhydropyrido [1,2-c]pyrimidine skeleton [21]. Modifications of 2a led to the development of a series of analogues with even more improved properties [13–16]. To improve the CCK1R binding properties of this family, it would be important to highlight the molecular mechanism and the functional ligand groups involved in the recognition process. Little is known about the complex mechanism by which these molecules are able to inactivate the CCK1R since no crystal structure of any complex has been obtained experimentally. Biological data obtained via rat CCK1R binding experiments [13–16] showed the importance of the hydrophobic character of the N-aryl group at position 2, the nature of the functional groups at the central pyridopyrimidine scaffold, and the fact that the (4aS,5R) configuration displays the highest degree of selectivity toward the CCK1R. Recently, site-directed mutagenesis [22] studies on the human CCK1R, permitted the identification of some amino acids involved in the recognition of pyridopyrimidine-based antagonists. These results revealed the importance of residues Asn333, Arg336, Ile329 and Ile352 in the recognition process, since mutation of these residues affected binding of the pyridopirimidine derivatives. Mutations also revealed the importance of residues Thr117 and Phe107. On the basis of these studies, a model for the complexes between compound 1a and the CCK1R was proposed [22]. This model allowed the binding site for the central scaffold and the N-aryl group at position 2 to be proposed, but did not accurately establish a defined position for the indole and Boc moieties [22].

In order to obtain more clues as to the character of the binding pocket of the Trp residue of these pyridopyrimidine derivatives, as well as to gain further insights into how the CCK1R recognizes the ligand, we set out to study a large set of pyridopyrimidine analogues using docking calculations to probe their binding modes and to highlight the main interactions with the receptor. Our calculations were supported by experimental data and special attention was given to residue Asn333, revealed as crucial in the recognition process of several agonists and antagonists of CCK1R [22, 23] including our derivatives. High affinity compounds with different substituents appended to the pyridopyrimidine skeleton were selected for the study, and compounds revealed as inactive by biological evaluation were also included. We were also interested in highlighting the features responsible for the diastereoelectivity of this family of compounds, by studying both active (4aS,5R)—and less active or inactive (4aR,5S)—diastereoisomers. Putative bioactive conformations obtained by automated docking could serve to explain the role of each functional group in the ligand and will be useful in optimizing its biological potency, opening new avenues in the development of novel potent CCK1R antagonists.

Materials and methods

CCK1R receptor

Like most other transmembrane G-protein coupled receptors, the high-resolution CCK1R structure has not been solved to date, thus only homology models can be used to perform docking studies. In the present paper, we use a CCK1R homology model that has already been presented and experimentally validated [24–27]. This structural model was built and refined progressively using a segmented approach in which the transmembrane helices, loop regions, N-terminus, and C-terminus were modeled as separated molecular entities on separate individual templates. The strategy incorporated experimental data based on the 3D structures of both bacteriorhodopsin and rhodopsin and from site-directed mutagenesis studies (details are given elsewhere [25]). The reliability of this CCK1R model was probed using molecular-dynamics simulations and free energy calculations in a realistic environment, indicating that both the structure of the receptor and its interactions

with the ligand are robust [26] and can be used in design studies [27]. Protein–ligand interactions found in the model, or reported in other studies, concerning the binding of different agonists and antagonists [28–31] highlighted some specific residues that are involved in the recognition process. Major anchoring points, which contribute 100- to 1,000-fold to the binding affinity constant of ligands to CCK1R are constituted by Arg197, Arg336 and Asn333. An N333A mutation clearly demonstrated the key importance of Asn333 in the recognition of the family of pyridopyrimidine-based CCK1R antagonists [22], as has also been observed for other agonists and antagonists of this receptor [23]. This single mutation leads to a total loss of activity. The data obtained also revealed that F107A, I329A, I329F, R336M and I352A mutations affect binding affinity.

Molecular structures and biological data of pyridopyrimidine-based antagonists

The structures and biological activities of the peptidomimetic ligands studied in this work [13–16] are listed in Fig. 1. These derivatives were selected to cover different chemical and structural aspects that might be important for binding to CCK1R. In these sense, pyridopyrimidine derivatives with different substituents at position 2 and 5 of the bicyclical ring have also been included, as well as compounds with modifications to the central scaffold. Experimental biological affinities are expressed as IC_{50}, which is the concentration of compound required to inhibit 50% of binding. Although the site-directed mutagenesis data used in this study were obtained using human CCK1R, we consider that the results are still valid for use with our series of compounds tested on rat CCK1R, as no sequence variation is seen between rat and human CCK1R within or near the binding site.

Two-dimensional structures of the ligands were drawn using the program ISISDRAW 2.5 [33], and the 3D structures correspond to the low energy state obtained after molecular-mechanics energy minimization with a minimum energy gradient of 0.01 kcal mol^{-1} Å^{-1} using the MM2 force-field available in the ChemOffice package [34].

Docking protocol

Docking simulations to locate the putative binding orientation and conformation of the compounds bound to the CCK1R were carried out using GOLD version 2.2 [35, 36]. The GA parameters used were the 3 times speed-up default parameter set offered in the GOLD2.2 front end, as recommended for very flexible ligands. The cavity was defined as all atoms within 10.0 Å of a single solvent-accessible point approximately at the center of the proposed active site from a model of compound 1a and CCK1R [22]. The radius cavity is large

enough to contain any possible binding mode of the very flexible ligands studied. The GOLD scoring function Chemscore [37] was applied to estimate the binding free energy change that occurs upon ligand binding.

In the absence of any crystal structure or experimental data on the 3D structure of any of the CCK1R-pyridopyrimidine-based ligand complexes, a target binding site was derived from our previous model of the [pyridopyrimidine **1a**-CCK1R] complex. Taking into account the fact that site-directed mutagenesis studies have shown that mutation of Asn333 of CCK1R leads to a total loss of affinity, docking calculations were carried out with an H-bond constraint between the key residue Asn333 and the ligand, without specifying the atom of the ligand. The 50 docked conformations obtained from the 50 GA for each ligand were extracted, and the best ranked conformations belonging to the top 15% were selected and analyzed.

Results and discussion

A detail comparison of the different docking solutions suggested that pyridopyrimidine ligands bind to the same binding pocket on the CCK1R; however, they can adopt two major conformations upon binding, which differ mainly in the 3D disposition of the *Boc* and indole moieties of the Trp residue.

The two possible binding conformations of the pyridopyrimidine derivatives can be illustrated by the complex between CCK1R and **1a**—we will refer to these two different models as mode I_A and mode I_B. In both modes, the ligand occupies the same pocket of the CCK1R receptor, located in a region comprising both extracellular loops and transmembrane helices (TM III, V, VI, and VII), as was shown in previous studies [22, 25]. The amino acids within 4Å of the docked ligand **1a** are shown in Fig. 2a. This figure shows that the active site is a "*Y*"-like shape composed of three pockets:

– The first pocket, P1, comprises mainly residues with hydrophobic aliphatic side chains, namely Gly122, Val125, Leu214, Ile329 and Ile352, together with an aromatic amino acid, Phe330. P1 also contains residue Asn333, shown by mutagenesis studies to be a key residue in the interaction with pyridopyrimidine-based antagonists, which can make H-bond contacts with the ligand.

– The second pocket, P2, also includes hydrophobic residues (Val43, Leu46, Ile108 and Val113); a residue, Phe107, with an aromatic side chain that is highly hydrophobic and can form a π-π stabilizing interaction with the ligand; Thr117, which contains an aliphatic chain with a hydroxyl group, which is more hydrophilic and reactive towards H-bond acceptors of the ligand;
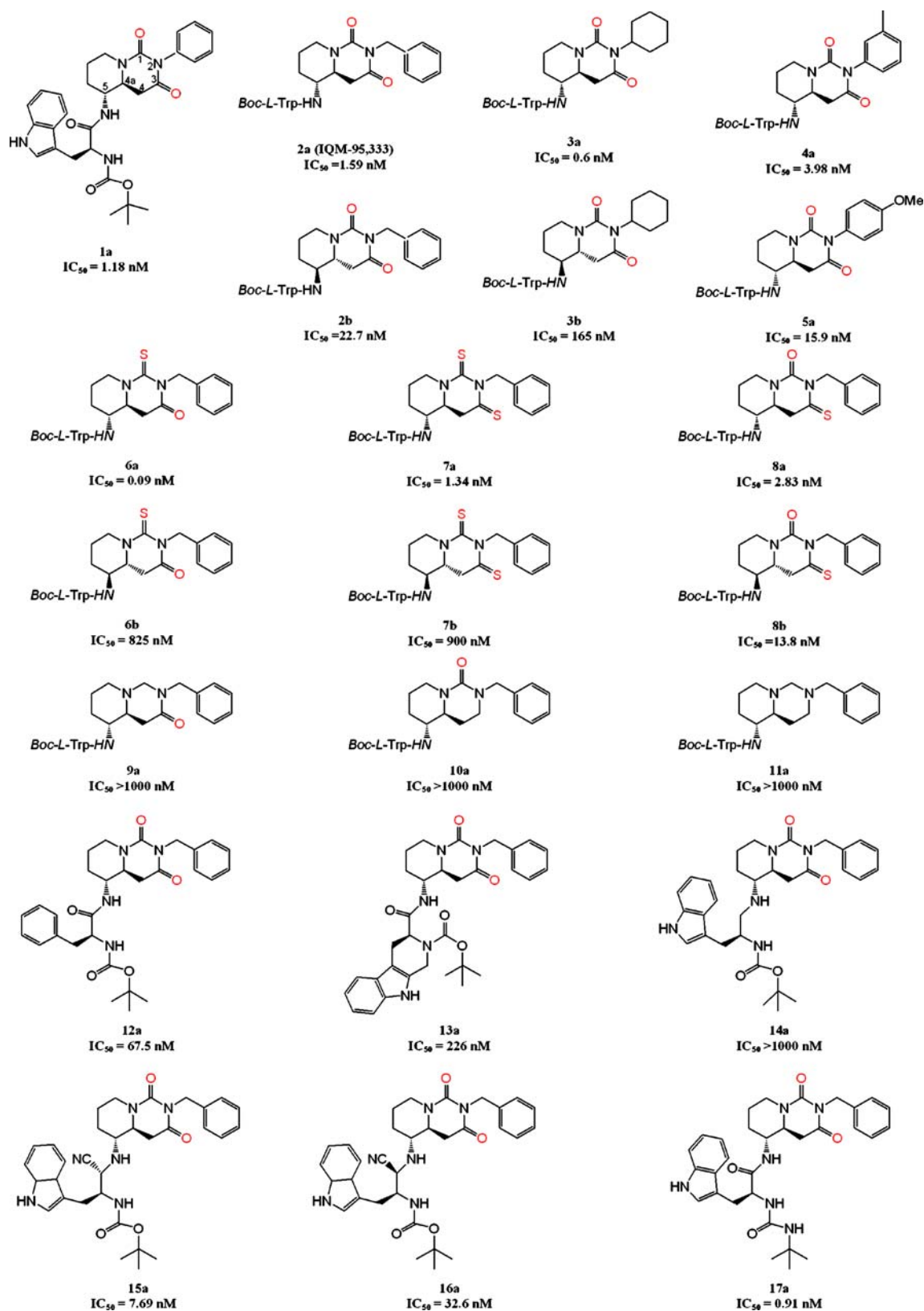
Fig. 1 Structures and experimental binding affinities, expressed as IC$_{50}$ values, of the pyridopyrimidine derivatives used in this study

Fig. 2 **a** Amino acids within 4Å of the modelled docked compound **1a** in the binding site of CCK1R. *Pink ribbon* Protein backbone, *orange cylinders* hydrophobic amino acids, *blue cylinders* hydrophilic amino acids. **b** Structure and anchoring sites of compound **1a**, as highlighted by SAR studies (for reasons of clarity, hydrogen atoms have been omitted)
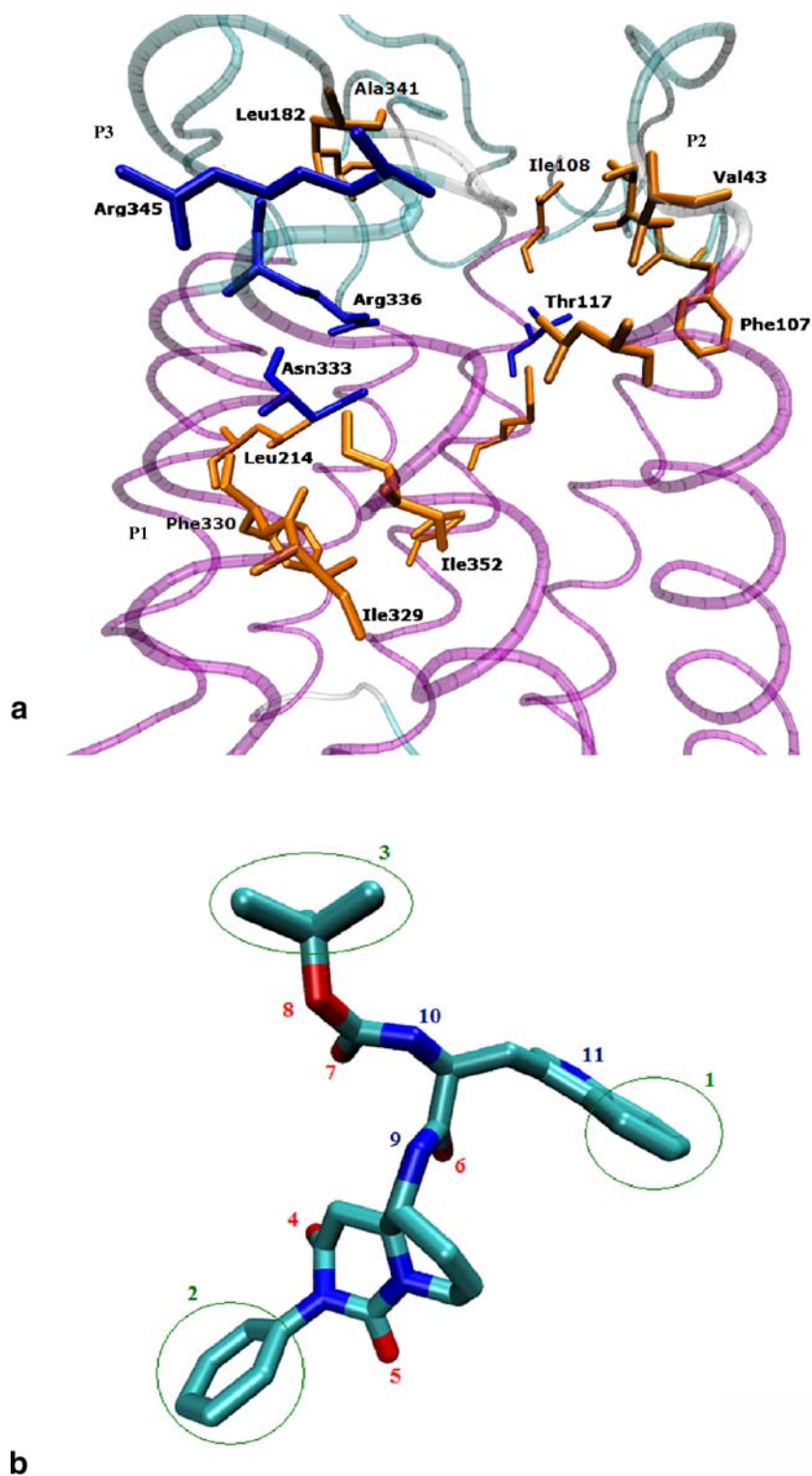
and Met121, which possess an aliphatic side chain with a hydrophobic thioether group.

– Pocket P3 is formed by hydrophobic residues Leu182, Ala337, Ala341and Ala343, and also contains hydrophilic amino acids, such as Arg336 and Arg345, with highly polar side chains.

Previous SAR studies [13–16] have suggested several putative anchoring points of compound **1a**, noted 1–11, which are depicted in Fig. 2b. Positions 1–3 are hydrophobic, positions 4–8 are H-bond acceptors, and positions 9–11 are H-bond donors. While the three external groups 1–3 favor binding with hydrophobic anchoring points in

the receptor, the peptide backbone and the central scaffold can make hydrogen-bond contacts with appropriate side chain residues of the binding site (Asn333, Arg336, Arg345 and Thr117). The high flexibility of the molecules, and the similar binding characteristics of each external arm, allow us to suppose that several binding modes are feasible.

In the two models obtained for [pyridopyrimidines-CCK1R] complexes I_A and I_B, the N-2 substituent and the central scaffold of the ligand fit similarly into the binding pocket, but the *Boc* and indole moieties are interchangeable. Figure 3 shows the superimposition of the two docking conformations obtained for compound **1a**. The rigid pyridopyrimidine scaffold and the N-aryl group are trapped in the top of transmembrane helices, whereas the more flexible *Boc*-Trp moiety can move into the flexible extracellular loops. The automated docking suggests that for both models I_A and I_B, the side chain of residue Asn333 is H-bonded to the carbonyl 3-CO of the pyridopyrimidine

scaffold (at position 4), in agreement with our previous model [22]. The methylene groups of the pyridopyrimidine scaffold are located in the vicinity of the side chains of Met121 and Leu46, leading to aliphatic hydrophobic interactions. The results also suggest putative hydrogen bonds between the backbone atoms of residues Ala343 and Val113 and the ligand. The N-2 hydrophobic substituent is located in the hydrophobic pocket P1 constituted by residues Val125, Leu214, Ile329, Phe330, and Ile352, and has a T-shape interaction with the aromatic side chain of residue Phe330. This interaction has also been observed for the C-terminal Phe of the natural ligand CCK.

In mode I_A, shown in Fig. 3a, Arg336 participates in an H-bond with the carbonyl group of the *Boc* moiety. The indole part of Trp is buried in the hydrophobic pocket (P2) containing Phe107 and Thr117, leading to π-π stabilizing interactions with the aromatic side chain of Phe107 and to an H-bond between the NH of indole and the carbonyl of residue Thr117. Moreover, the backbone CO of Ala343 and
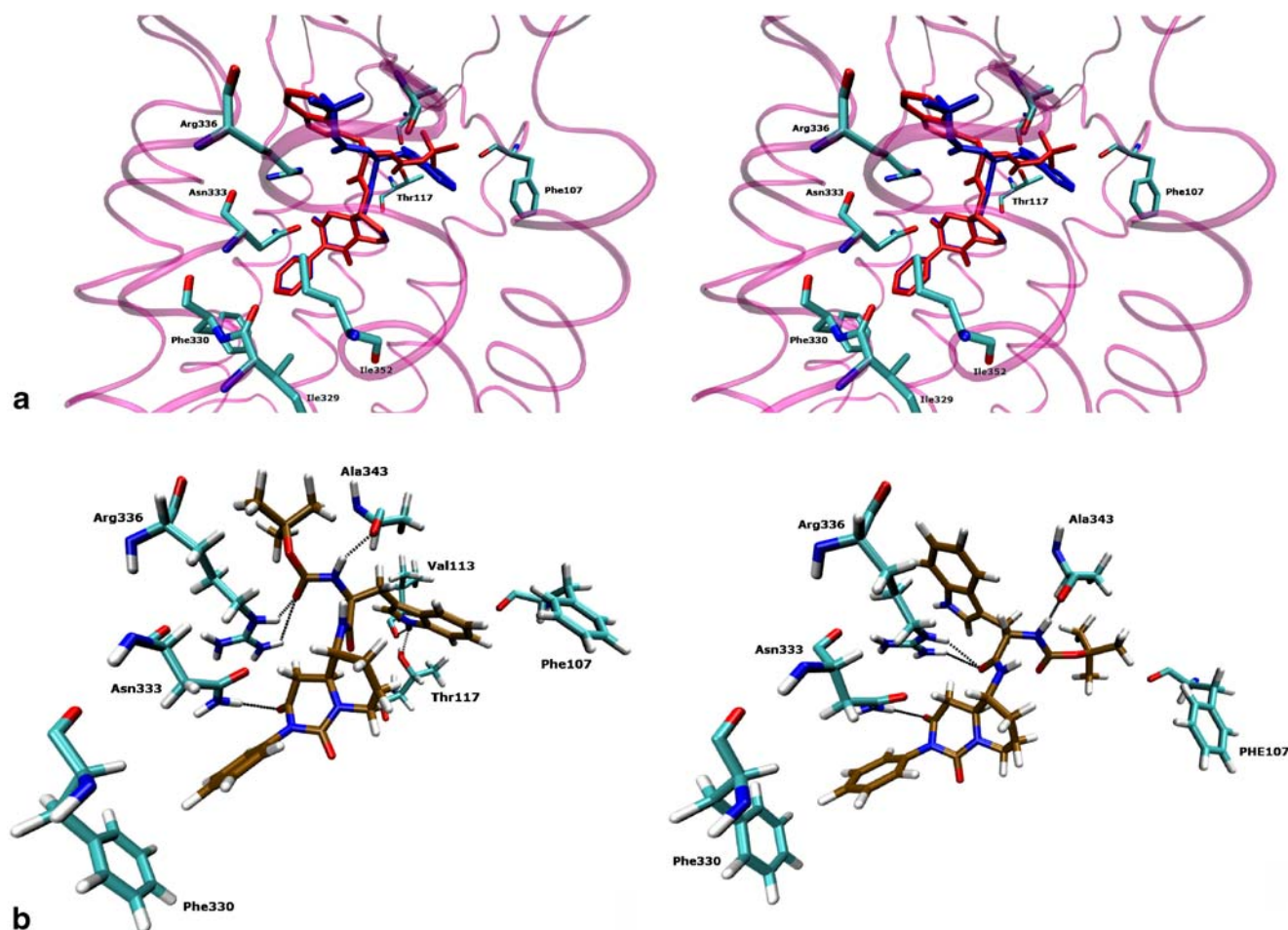

Fig. 3 A stereo view of the two possible binding conformations for compound **1a** obtained by molecular docking: binding modes I_A (in *blue*) and I_B (in *red*). For reasons of clarity only interacting residues of the active site are highlighted and hydrogen atoms are omitted. *Pink* *ribbon* shows Protein backbone. Hydrogen bond interactions of compound **1a** in binding modes I_A (shown in **a**) or I_B (shown in **b**) at the active site of CCK1R

Val113 are linked to the ligand via hydrogen bonding with the NH groups of the *Boc* moiety and the indole ring, respectively. The *tert*-butyl group of the *Boc* moiety is in the vicinity of hydrophobic residues Val341 and Leu182, leading to aliphatic hydrophobic contacts.

In mode I_B, there is also an H-bond with the side chain of Arg336 as in model I_A, but the H-bond acceptor differs, with the carbonyl group of the Trp moiety being involved as shown in Fig. 3b. Additionally, the NH group of the *Boc* moiety forms an H-bond with the backbone CO of Ala343. The indole part of Trp is buried in pocket P3, constituted by residues Arg345, Thr340, Ala337, Leu182 and Ser342.

Representations of the selected binding modes of the derivatives that are most structurally representative of this family are given in Figs. 3, 4, 5, and 6. Binding mode details are described in the following sections.

Compounds with (4aS,5R) stereochemistry (Compounds a)

Analysis of the data for the (4aS,5R)-isomers showed two possible binding conformations for these pyridopyrimidine derivatives, as for compound **1a**. However, some derivatives showed preferences for one of the binding conformations, and the existence of a unique binding conformation was even detected in some cases. In this sense, although models I_A and I_B are both present within the top-ranked solutions for compound **1a**, the most favorable conformation belonging to the most populated binding mode corresponds to I_B, in which the carbonyl of the tryptophan moiety is hydrogen bonded to Arg336. This result is in agreement with a model previously proposed for this compound obtained from molecular dynamic calculations [22].

Modifications at the N-2 position: compounds 2, 3, 4, and 5

Compound **2a**, with a benzyl group at position 2 of the pyridopyrimidine skeleton, binds preferably in mode I_A. In the top 15% of solutions, only one conformation, in which

residue Thr117 is linked to the carbonyl of the *Boc* moiety, belongs to mode I_B. The estimated docking binding affinities are in agreement with this result and indicate that the pose in mode I_A is more favorable than in I_B. Replacement of benzyl in **2a** by a cyclohexyl as in **3a** increases the binding potency. All the docking poses of this compound were similar to those reported for **2a**, and belong to binding conformation I_A, with the same set of interactions. However, unlike **2a**, in all poses, the carbonyl group of the Trp moiety is about 3.9 Å from the donor residue Arg336, suggesting that a slight rotation in this part of the molecule can lead to formation of an additional H-bond with the NH of residue Arg336. This feature, as well as the higher lipophilic character of the N-2 substituent (*log*P=2.148 for **3a** and 1.822 for **2a**), could explain the subnanomolar potency of **3a** compared to **2a**. The cyclohexane ring should form stronger hydrophobic interactions with pocket P1 containing Ile329 and Ile352. Visualization of the binding position reveals that the H-bond with residue Asn333 is shorter in **3a** than in **2a** (3.188 Å and 3.251 Å, respectively). Experimental data concerning the introduction of an electron-donating substituent on the phenyl group of **1a**, as in compounds **4a** and **5a**, led to a slight and moderate decrease in the binding affinity, respectively. The obtained poses of compounds **4a** and **5a** in the active site are similar to **3a** in mode I_A. Visualization of the selected conformations (see Fig. 4) shows that the two conformations are easily superimposable. However, in compound **5a**, the T-shaped interaction of the N-2 substituent with Phe330, at the bottom of pocket P1, is characterized by higher steric hindrance if the group is introduced in the *para*- position (the methyl group is 2.70 Å and 2.433 Å away from the phenyl of residue Phe330 and the methyl of residue Ile329, respectively) than when it is in the *meta*- position compound **4a** (the methyl group is 3.636 Å and 3.391 Å away from the phenyl of residue Phe330 and the methyl of residue Ile329, respectively). The position and spatial orientation of the introduced group could explain the
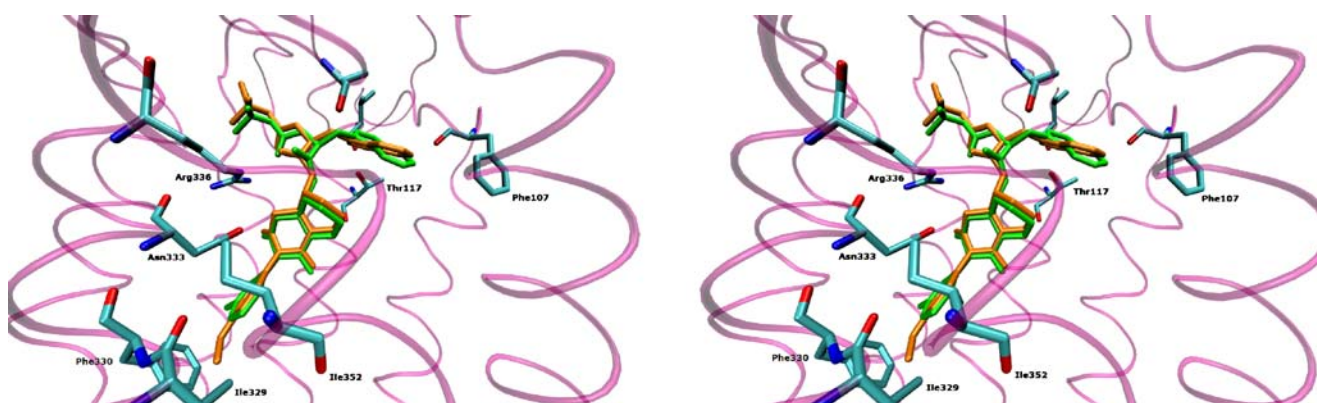

Fig. 4 A stereo view superimposing the docking conformations of compounds **4a** (in *green*) and **5a** (in *orange*) within the CCK1R model

difference between the observed experimental binding affinities of these two compounds.

Modifications of the central scaffold: compounds 6, 7, and 8

Docking of thiocarbonyl compound **6a** leads to the isopopulated modes I_A and I_B. The more favorable binding mode is I_A, whereas the I_B-like models appears within the top 15%, but lower in rank and characterized by the absence of the interaction with Arg336. Visualization of the selected pose shows that the thioxo group of the central scaffold points towards the hydrophobic pocket P1 (see Fig. 5). We speculate that the sulfur atom, which is more lipophilic than the oxygen, establishes additional favorable hydrophobic contacts in pocket P1 that allow us to explain the subnanomolar affinity of this compound. This interaction is favored by a longer C=S bond compared to the C=O bond (1.586 Å and 1.209 Å, respectively). The same binding conformation is obtained with compounds **7a** and **8a** in mode I_A, which are easily superimposed on compound **2a**, whereas compound **6a** seems to fit better with the hydrophobic pocket P1. Since the 3-CO is the carbonyl involved in an H bond with the protein in our models, another possible explanation of the increased affinity of the thio derivative **6a** (3-CO) compared to **7a** and **8a** (3-CS) might be the stronger H-bond between the carbonyl at position 3, as in **6a**, compared to the H-bond with the thiocarbonyl group. Additionally, the higher affinity of the thiocarbonyl compound **6a** in comparison to its carbonyl counterpart **2a** might be attributed to a decrease in the solvation energy in solution of the thiocarbonyl group.

Reduction of the central scaffold: compounds 9, 10, and 11

Experimental data show that the reduced compounds **9a**, **10a** and **11a** do not bind to the CCK1R. Only three conformations are obtained in the top-ranked solutions for compound **9a**. The two highest ranked solutions correspond to mode I_A, in which the H-bond with Asn333 is formed with the 3-CO carbonyl, as in compound **2a**. However, the central pyridopyrimidine scaffold occupies a region of the binding pocket that is free in other active compounds, suggesting steric hindrance in this region of the pocket that likely results in a less stable complex, leading to a loss of affinity for CCK1R. The third conformation, corresponding to mode I_B, is characterized by the absence of the H-bond with residue Asn333—reorientation and twisting of the N-2 group results in the occupation of a position that is free in active compounds, and out of the hydrophobic pocket P1. Figure 6a shows the superimposition of the two compounds **2a** and **9a** in mode I_A. On the other hand, the docking solutions of compound **10a** led to the most populated cluster in mode I_A. It shows a position of the central scaffold closer to the disposition adopted in compound **2a** but due to the lack of the 3-CO group it is unable to form a hydrogen bond with the Asn333 residue (see Fig. 6b). The slight difference in the estimated binding energies of the two binding poses for **9a** and **10a** could suggest that these compounds swing between these two binding modes and could indicate instability of their binding into the pocket. Docking of the reduced compound **11a** resulted in only one binding position (shown in Fig. 6c) in the top 15%, similar to mode I_A. However, docking failed to find any H-bond with the ligand despite the presence of carbonyl groups in the Boc and Trp moieties, which can explain the loss of
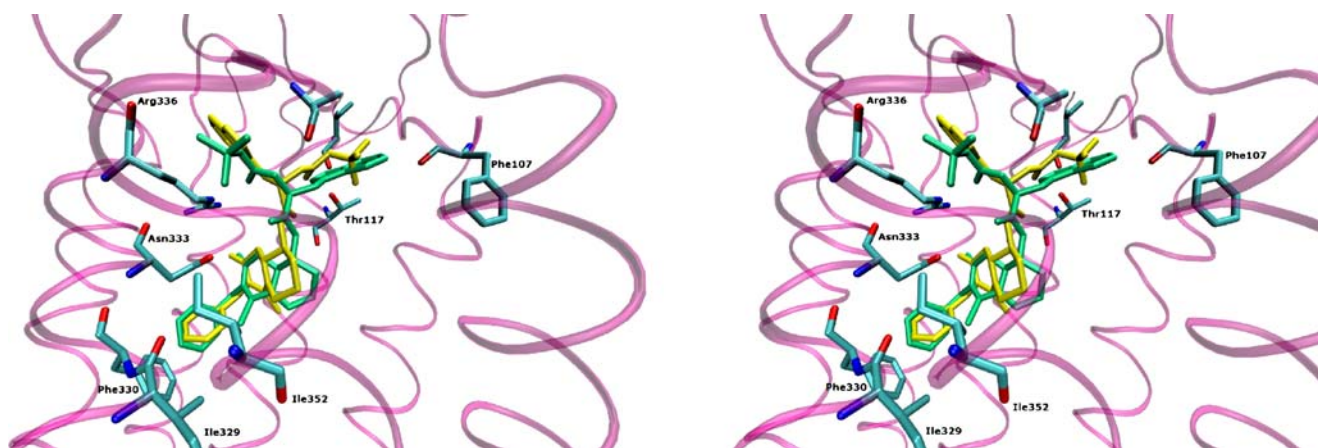

Fig. 5 A stereo view superimposing the docking conformations for compound **6a** (in *green*) and its isomer **6b** (in *yellow*) within the CCK1R model
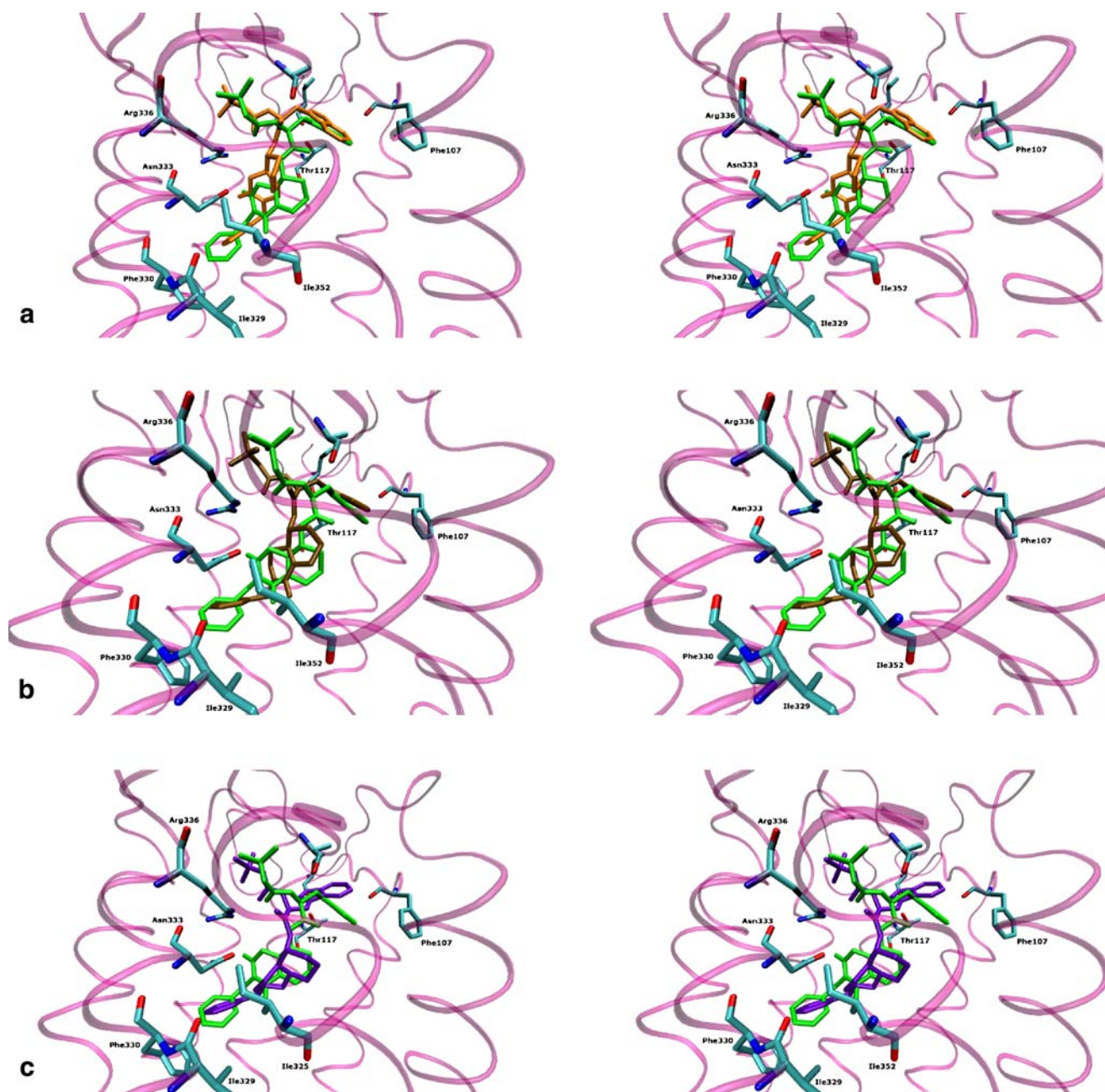
Fig. 6 Stereo views of superimposition of docking conformations. **a** Compound **1a** (in *green*) and **9a** (in *orange*), **b** compound **1a** (in *green*) and **10a** (in *brown*), **c** compound **1a** (in *green*) and **11a** (in *purple*)

activity. Visualization of the selected binding conformations shows that, because of the lack of carbonyls on the central scaffold and the loss of its planarity, the new topography of the central scaffold lead to poor contacts between the methylene groups and some residues of the pocket (2.9 Å from Leu46 and 2.6Å from Ile352), as shown in Fig. 6c. Steric hindrance and the lack of the key interaction suggest that this compound will form an unstable complex with the receptor and could explain the loss of activity observed experimentally.

Docking of compounds **9a** and **10a** confirms that the two carbonyls of the central scaffold do not have the same chemical role in the binding mechanism. Thus, visualization of the selected conformations shows that the docked conformations superimpose well at the N-2 group and *Boc*-Trp moiety, whereas the positions of the central scaffold are different. The 3-CO is an H-bond acceptor position, whereas the 1-CO seems to play a role in maintaining the three-dimensional shape of the central scaffold.

Modifications of tryptophan moiety: compounds **12**, **13**, **14**, **15**, **16**, *and* **17**

Docking of compound **12a**, obtained by replacement of the indole group in the tryptophan moiety by a phenyl moiety, leads to the top conformations, all of which are in mode I_B. The selected conformation is characterized by the absence of the interaction with the residue Arg336 that was shown to be important. The lack of this interaction could explain the moderate activity of this compound observed experimentally.

The conformational restriction introduced by the tetrahydro-β-carboline system into compound **13a** leads to a decrease in its flexibility. As a consequence, all the obtained binding poses are in mode I_A. However, the predicted bioactive conformation lacks the key interaction with residue Asn333. The lack of this H-bond might explain the poor activity observed experimentally for this compound, even if an additional H-bond between the carbonyl group of the Trp moiety and residue Arg336 is established.

In compound **14a**, the carboxamide bond of the Trp moiety is replaced by a reduced peptide bond, leading to a total loss of activity. Docking calculations resulted in two isoenergetic binding modes, I_A and I_B, both characterized by the fact that the central scaffold occupies a region of the pocket that is usually free in active compounds. Because of the lack of the Trp carbonyl moiety, the ligand is more folded into the pocket compared with compound **2a**. Because of the sp^3 hybridization of the reduced carbon, the backbone angle values in the Trp part are 109°, 116° for **14a** compared to 114°, 122° for compound **2a**. As a consequence, a change in the position of the pyridopyrimidine double ring leads to steric hindrance in the pocket and leads to the loss of the interaction with residue Asn333 in **14a**. The distance between the side-chain NH hydrogen of Asn333 and the 3-CO carbonyl group is then longer (4.077 Å and 2.912 Å, respectively for **14a** and **2a**). These features may explain the loss of activity of compound **14a**.

Docking of compound **15a** leads to one binding conformation in mode I_B in the top ranking, in which a hydrogen bond is established between the CN of the R-[CH(CN)NH] group of the Trp moiety and residue Arg336. This latter interaction is absent in the isomer S-[CH(CN)NH], **16a**, which binds favorably in the I_A mode. This can explain its moderate activity compared to compound **15a**.

The two binding modes I_A and I_B were observed in the top rankings for compound **17a** with the same population, as was obtained for the subnanomolar compound **6a** in mode I_A. Two hydrogen bonds are established between residue Arg336 and the ligand (CO of *Boc* and, in mode I_B, an H-bond is established between the CO of Trp and Arg336). In mode I_A, the selected conformation can be well superposed on the conformation obtained in the case of compounds **6a** and **7a**, which also show subnanomolar

binding affinity. In the obtained models I_A and I_B, binding position 8 of the ligand is not linked to the protein. The replacement of the urethane *N-Boc* protection of **2a** by the *tert*-butylaminocarbonyl group in compound **17a** had no significant effect experimentally upon the affinity. This is in agreement with our selected docking conformation.

Compounds with (4aR,5S) stereochemistry: **2b**, **3b**, **6b**, **7b**, *and* **8b**

Experimental binding affinities have shown that although some (4aR,5S)-pyridopyrimidines (**b** compounds) have good binding affinities for CCK1R, in general there is a decreases in affinity [14, 15]. The analysis of docking data shows that they can also adopt the two binding conformations in mode I_A or I_B as obtained for the (4aS,5R)-isomers (**a** compounds).

Docking of isomer **2b** led to similar results as **1a**: two feasible binding modes I_A and I_B. However, mode I_B is predominant and characterized by an H-bond interaction between the carbonyl of the *Boc* group and residue Arg336, as was obtained for compound **1**. An interesting result was obtained by docking the inactive (4aR,5S)-isomer **6b**. As shown in Fig. 5, the binding pose for **6b** is similar to that observed for mode I_B, with the lack of the interaction with residue Arg336. In addition, the (4aR,5S) configuration of the central scaffold prevents the thioxo group from pointing towards the hydrophobic pocket P1, which can explain the decrease in affinity of compound **6b** in comparison with **2b**. In this sense, the larger volume of the sulfur atom compared to the oxygen is in a region of the receptor that is free in active compounds, being about 2.5 Å from residues Met121 and Val125, yielding to steric hindrance and close contacts.

The same results were obtained with compounds **7b** and **8b**, which bind favorably and exclusively, respectively, in mode I_B, and also lack the interaction with Arg336.

In the case of compound **3b**, all the obtained binding positions are similar to the positions of its isomer **3a** in mode I_A with the same set of interactions. However, visualization of the two superimposed conformations shows that isomer **3b** occupies a region of the pocket that is free in the case of **3a**. We speculate that this position yields to steric hindrance and thus the compound would be less well retained by the receptor.

Prediction of binding free energy

The predicted binding free energies ($\Delta G_{binding}$), given by the Chemscore, of the selected conformations for both (4aS,5R)- and (4aR,5S)- isomers in the two modes I_A and I_B, and the corresponding experimental pIC_{50} (co-logarithm of IC_{50}) values are listed in Table 1. The putative active conformation (in bold) corresponds to the predominant

Table 1 Experimental pIC_{50} and estimated binding free energy ($\Delta G_{binding}$) of the more favorable binding modes I_A and I_B, obtained for each compound (putative active conformations are in bold)

Compound	Experimental pIC_{50}[a]	Chemscore $\Delta G_{binding}$ (kJ mol^{-1})	
1a	− 0.071	I_A :	− 41.46
		I_B :	**− 45.52**
2a (IQM-95,333)	− 0.201	**I_A** :	**− 48.42**
		I_B :	− 41.45
2b	− 1.356	I_A :	− 46.93
		I_B :	**− 43.27**
3a	0.221	**I_A** :	**− 48.92**
		I_B :	− 48.42
3b	− 2.217	**I_A** :	**− 41.71**
4a	− 0.599	**I_A** :	**− 49.48**
		I_B :	− 46.47
5a	− 1.201	**I_A** :	**− 48.33**
6a	1.045	**I_A** :	**− 48.32**
		I_B :	− 42.96
6b	− 2.916	I_A :	− 47.06
		I_B :	**− 45.41**
7a	− 0.127	**I_A** :	**− 50.21**
		I_B :	− 45.49
7b	− 2.954	I_A :	− 49.92
		I_B :	**− 44.31**
8a	− 0.451	**I_A** :	**− 49.23**
		I_B :	− 45.32
8b	− 1.139	**I_B** :	**− 44.06**
9a	IN[b]	**I_A** :	**− 46.72**
		I_B :	− 45.83
10a	IN	**I_A** :	**− 50.22**
		I_B :	− 50.75
11a	IN	**I_A** :	**− 49.40**
12a	− 1.829	**I_B** :	**− 38.72**
13a	− 2.354	**I_A** :	**− 45.61**
14a	IN	**I_A** :	**− 47.21**
15a	− 0.885	**I_B** :	**− 43.95**
16a	− 1.513	**I_A** :	**− 44.16**
17a	0.041	**I_A** :	**− 51.87**
		I_B :	− 45.92

[a] $pIC_{50} = -\log(IC_{50})$
[b] Inactive compound

mode in the analyzed set of docked conformations. The values in the table show that, in general, (4aS,5R) isomers prefer binding in mode I_A, which is predominant compared to I_B, in accordance with the values of $\Delta G_{binding}$ estimated by Chemscore for mode I_A compared to mode I_B. It is interesting to note that the significant differences between $\Delta G_{binding}$ given by the scoring function Chemscore for both **a** and **b**, in general showed greater affinity for **a** derivatives. This result could suggest that the CCK1R is able to discriminate between the two isomers, providing a possible explanation for the chiral selecting behavior displayed by this receptor towards the studied compounds. However, a poor correlation (R=0.630) was obtained between experi-

mental pIC_{50} and Chemscore $\Delta G_{binding}$ of the studied compounds, as shown in the plot in Fig. 7. Although GOLD has been shown to have a success rate of 75% for predicting the binding mode of compounds with about 8–12 rotational bonds, the empirical GOLD fitness functions were designed to discriminate between different binding modes of the same molecule. Few correlations have been observed between GOLD fitness scores and biological activity, illustrating the difficulty of using GOLD to discriminate structurally similar and extremely hydrophobic compounds [38, 39], as is the case in the present study.

The ligand–receptor interaction is mediated by other factors such as the flexibility and conformational changes of the receptor during binding with the ligand, which is one of the major difficulties in predicting protein–ligand complexes [40, 41]. However, in the version of GOLD used here, only dihedrals of protein OH and NH_3^+ groups are optimized and the protein backbone is not flexible [42]. These features may also explain the poor correlation obtained. It can also be attributed to the use of a theoretical model of the receptor and the absence of any experimental data on the position of the ligand into the pocket to make a comparison with an observed position and test the effectiveness of the docking protocol.

Conclusions

In the current study, we used automated molecular docking to study the binding pocket of a series of pyridopyrimidine-based CCK1R antagonists. The results have allowed us to provide a plausible explanation of the different binding affinities observed by highlighting the most important interactions with CCK1R. These results are in agreement with previous site-directed mutagenesis
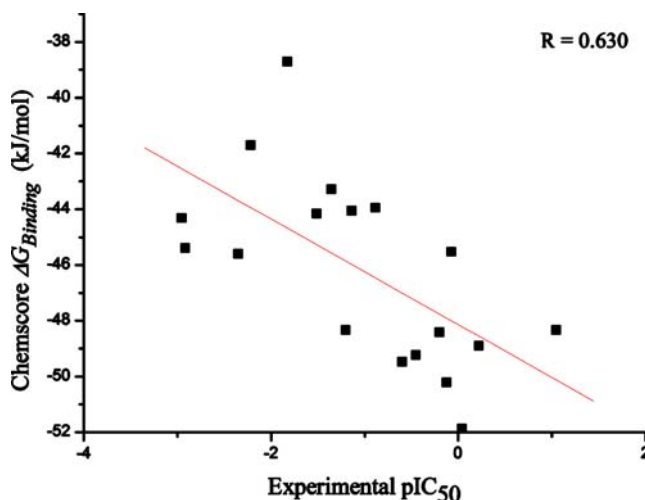

Fig. 7 Plot of Chemscore-estimated binding free energies ($\Delta G_{binding}$) vs experimental pIC_{50} [$-\log(IC_{50})$]

studies and structure–activity relationships on pyridopyrimidine derivatives [22].

According to the docking data, these antagonists occupy the top of the transmembrane helices and extracellular loops, as has been observed for other non-peptide antagonists. The binding site consists of three main pockets, composed mostly of hydrophobic amino acids that can accommodate the lipophilic arms of the studied compounds. The presence of the hydrophilic amino acids Thr117, Asn333, Arg336 and Arg345 may also be responsible for recognition through H-bond interactions. The automated docking found, for this family of antagonists, one binding pocket in which the ligand can bind in two different conformations, modes I_A and I_B, which differ essentially in the position of the *Boc* and indole groups of the Trp residue in binding pockets P2 and P3. This result is not surprising given the great flexibility of the *Boc*-Trp moiety, which is bound to the flexible extracellular loops of CCK1R, as well as the similar physico-chemical properties of the two arms of this part of the ligand. It is interesting to note the importance of the central scaffold, which fits rather well into the transmembrane helices, and is able to provide the correct 3D disposition to the substituents at position 2 and 5.

On the whole, our results have allowed us to explore the probable binding conformations of pyridopyrimidine derivatives at the active site of the CCK1R, and also provide some useful indications for understanding the chemical features that govern the very complex mechanism of inactivation of this receptor. This knowledge will help in the rational design of new CCK1R ligands, with potential application in feeding disorders.

References

1. Royer CA (1995) Biophys J 68:1191–1195
2. Fang K (1999) New photoaffinity labeling protocol for studying ligand-receptor interactions. Dissertation, Columbia University
3. Gurd FRN, Wittebort RJ, Rothgeb TM, Neireiter J Jr (1983) Motions of aliphatic residues in Myoglobins. In: Bothner-By AA, Glickson JD, Sykes BD (eds) Biochemical structure determination by NMR. Dekker, New York
4. Bourgeois D, Royant A (2005) Curr Opin Struct Biol 15:538–547
5. Miao J, Chapman HN, Kirz J, Sayre D, Hodgson KO (2004) Annu Rev Biophys Biomol Struct 33:157–176
6. Hassan SA, Gracia L, Vasudevan G, Steinbach PJ (2005) Methods Mol Biol 305:451–492
7. Veselovsky AV, Ivanov AS (2003) Curr Drug Targets: Infect Disord 3:33–40
8. Anderson AC (2003) Chem Biol 10:787–797
9. Henry CM (2001) Pharmaceuticals 79:69–74
10. Wank SA (1995) Am J Physiol 269:G628–G646
11. Noble F, Wank SA, Crawley JN, Bradwejn J, Seroogy KB, Hamon M, Roques BP (1999) Pharmacol Rev 51:745–781
12. Wank SA (1998) Am J Physiol 274:G607–G613
13. Martinez M, Bartolomé-Nebreda JM, Gomez-Monterrey I, Gonzalez-Muniz R, Garcia-Lopez MT, Ballaz S, Barber A, Fortuno A, Del Rýo J, Herranz R (1997) J Med Chem 40:3402–3407
14. Bartolomé-Nebreda JM, Patino-Molina R, Martin-Martinez M, Gomez-Monterrey I, Garcýa-Lopez MT, Gonzalez-Muniz R, Cenarruzabeitia E, Latorre M, Del Rýo J, Herranz R (2001) J Med Chem 44:2219–2228
15. Bartolomé-Nebreda JM, Garcýa-Lopez MT, Gonzalez-Muniz R, Cenarruzabeitia E, Latorre M, Del Rýo J, Herranz R (2001) J Med Chem 44:4196–4206
16. Bartolomé-Nebreda JM, Gomez-Monterrey I, Garcýa-Lopez MT, Gonzalez-Muniz R, Martin-Martinez M, Ballaz S, Cenarruzabeitia E, LaTorre M, Del Rýo J, Herranz R (1999) J Med Chem 42:4659–4668
17. Crawley JN, Corwin RL (1994) Peptides 15:731–755
18. Moran TH (2000) Nutrition 16:858–865
19. Herranz R (2003) Med Res Res 23:559–605
20. Dunlop J (1998) Gen Pharmacol 31:519–524
21. Ballaz S, Barber A, Fortunòo A, Del Río J, Martín-Martínez M, Gómez-Monterrey I, Herranz R, González-Munòiz R, García-López MT (1997) Br J Pharmacol 121:759–767
22. Martin-Martinez M, Marty A, Jourdan M, Escrieut C, Archer E, Gonzalez-Muniz R, Garcia-Lopez MT, Maigret B, Herranz R, Fourmy D (2005) J Med Chem 48:4842–4850
23. Gigoux V, Escrieut C, Fehrentz J-A, Poirot S, Maigret B, Moroder L, Gully D, Martinez J, Vaysse N, Fourmy D (1999) J Biol Chem 274:20457–20464
24. Archer E, Maigret B, Escrieut C, Pradayrol L, Fourmy D (2003) Trends Pharmacol Sci 24:36–40
25. Archer-Lahlou E, Tikhonova I, Escrieut C, Dufresne M, Seva C, Pradayrol L, Moroder L, Maigret B, Fourmy D (2005) J Med Chem 48:180–191
26. Hénin J, Maigret B, Tarek M, Escrieut C, Fourmy D, Chipot C (2006) Biophys J 90:1232–1240
27. Tikhonova IG, Marco E, Lahlou-Archer E, Langer I, Foucaud M, Maigret B, Fourmy D (2007) Curr Top Med Chem 7:1243–1247
28. García-López MT, González-Muñiz R, Martín-Martínez M, Herranz R (2007) Curr Top Med Chem 7:1180–1194
29. Noble F (2007) Curr Top Med Chem 7:1173–1179
30. Gigoux V, Maigret B, Escrieut C, Silvente-Poirot S, Bouisson M, Fehrentz JA, Moroder L, Gully D, Martinez J, Vaysse N, Fourmy D (1999) Protein Sci 8:2347–2354
31. Escrieut C, Gigoux V, Archer E, Verrier S, Maigret B, Behrendt R, Moroder L, Bignon E, Silvente-Poirot S, Pradayrol L, Fourmy D (2002) J Biol Chem 277:7546–7555
32. Gouldson P, Legoux P, Carillon C, Delpech B, Le Fur G, Ferrara P, Shire D (2000) Eur J Pharmacol 400:185–194
33. ISIS DRAW 2.5 (2002) MDL Information Systems, San Leandro, CA
34. CS Chem Office, Ultra Microsoft Windows, Cambridge Scientific Computing, Cambridge, MA
35. Jones G, Willett P, Glen RC (1995) J Mol Biol 245:43–53
36. Jones G, Willett P, Glen RC (1997) J Mol Biol 267:727–748
37. Eldridge MD, Murray CW, Auton TR, Paolini GV, Mee RP (1997) J Comput-Aided Mol Des 11:425–445
38. Stewart KD, Bently JA, Cory M (1990) T C Methods 3:713
39. Holt DA et al (1993) J Am Chem Soc 115:9925
40. Teague SJ (2003) Nature Rev Drug Discov 2:527–541
41. Gunasekaran K, Nussinov R (2007) J Mol Biol 365:257–273
42. Verdonk ML, Cole JC, Hartshorn MJ, Murray CW, Taylor RD (2003) Proteins 52:609–623